

## Gold nanoparticle-based sensing strategies for biomolecular detection\*

Lihua Wang, Shiping Song, Dun Pan, Di Li, and Chunhai Fan<sup>‡</sup>

*Division of Physical Biology, Shanghai Institute of Applied Physics, Chinese Academy of Sciences, Shanghai 201800, China*

*Abstract:* Gold nanoparticles (AuNPs) have been extensively employed in biological studies for several decades. More recently, progress has well demonstrated that DNA-conjugated AuNPs are highly promising nanoprobes for the sensitive detection of various biomolecules, based on the unique optical and electronic properties of AuNPs. In this short review, we focus on the use of AuNP-based nanoprobes for biological detection of nucleic acids, proteins, and other biologically relevant small-molecule targets, mainly based on the recent progress in our laboratory.

*Keywords:* biosensors; DNA; gold nanoparticles; nanoprobes; surface plasmon resonance.

### INTRODUCTION

There have been ever-growing demands to develop rapid, field-portable, and cost-effective devices for a wide range of applications such as biomedical diagnostics, food safety and environmental monitoring, forensic analysis, and civil defense. Aiming at such goals, the development of biosensors has received intense research and industrial interest. Biosensors are analytical devices that convert biological recognition events into measurable physical signals, which take advantage of the marriage between Nature-endowed highly specific biomolecular interactions and advanced optoelectronic transducers. More recent progress has well demonstrated that nanotechnology offers unique opportunities for the development of novel, highly sensitive biosensing devices [1,2]. Particularly, nanomaterials with at least one size dimension in the size range of 1–100 nm [3] have been popularly employed in various biosensing designs to meet challenges that were otherwise impossible with currently available technologies. Nanomaterials are of the size dimension between atoms and bulk materials, and possess many unique and attractive features, such as high surface-to-volume ratio [3–7], quantum size effect [8], and electrodynamic interactions [9].

We are particularly interested in the use of gold nanoparticles (AuNPs) to improve the performance of biomolecular detection. AuNPs are well known to be biocompatible, which is an essential feature for the coupling of DNA and proteins with this nanomaterial. Also, importantly, AuNPs are of approximately the same dimension with biomolecules and possess unique optical and electronic properties [10–18]. In fact, the use of AuNPs has a long history in biology, dating back to the application of “immunogold” in biological imaging in the 1970s. More recently, since the pioneering work of Alivisatos and Mirkin in 1996 [19,20], the site-specific attachment of DNA probes on AuNPs based on well-established gold-thiol chemistry has led a large number of AuNP-based biological probes. Here,

---

\*Paper based on a presentation at the 13<sup>th</sup> International Biotechnology Symposium (IBS 2008): “Biotechnology for the Sustainability of Human Society”, 12–17 October 2008, Dalian, China. Other presentations are published in this issue, pp. 1–347.

<sup>‡</sup>Corresponding author: E-mail: fchh@sinap.ac.cn

we will briefly review the design of AuNP-based probes for biological detection of a range of nucleic acid and protein targets, mainly based on the recent progress in our own laboratory.

AuNPs possess several combined advantages as nanoprobe for biodetection. First, AuNPs are easily synthesized via chemical reduction, with excellent mono-dispersity. More importantly, AuNPs can be readily chemically modified with thiols, including thiolated DNA probes. Second, AuNPs have high extinction coefficient, which make them highly promising colorimetric probes. AuNPs exhibit a strong surface plasmon resonance (SPR) absorption band in the visible region [21,22], which arises from the coherent electron oscillation of surface gold atoms induced by the incident electromagnetic field [3,23,24]. As a result, small AuNPs (e.g., 10 nm in diameter) absorb green light, corresponding to a strong SPR absorption band at ~520 nm in the visible light spectrum, and the solution appears red in color. Third, aggregated AuNPs turn the solution color to purple or blue due to the inter-particle plasmon coupling [25]. This characteristic red-to-blue color change of AuNPs has been extensively employed to develop a range of biomolecular detection methods. Fourth, AuNPs possess many unique optical and electronic properties. For example, AuNPs are superquenchers for almost all fluorophores; and AuNPs are excellent conductors. Fifth, AuNPs are biocompatible, making them ideal platforms for the immobilization of biomolecules. Also, importantly, the large surface-to-volume ratio allows one particle to carry a number of biomolecules. In this review, we will first describe recent work on AuNP/DNA conjugates as nanoprobe for biomolecular detection, and then unmodified AuNP probes.

### AuNP/DNA CONJUGATES AS NANOPROBES

AuNPs can be readily modified with thiolated DNA probes via the Au-S chemistry-based self-assembly. In 1996, Alivisatos and Mirkin reported the construction of AuNP/DNA conjugates by functionalizing AuNPs with thiol-modified oligonucleotides in their pioneering work almost at the same time [19,20]. Thus prepared AuNP/DNA conjugates usually have a high density of DNA monolayer (e.g., over 200 probes on a 13-nm AuNP [26]), with DNA molecules protruding into the solution. Since DNA molecules are highly charged polyelectrolytes, these conjugates are extremely stable in solution, and retain the mono-dispersity in solutions of very high ionic strength (e.g., >1 M NaCl). These discoveries led to various biological detection scheme based on AuNP/DNA conjugates [27,28].

In a typical design, AuNPs are modified with two kinds of DNA probes that are complementary to different parts of the target DNA (Fig. 1A). Thus, in the presence of target DNA, two AuNP probes are cross-linked with the target molecules to form a network, i.e., AuNP aggregates. This target-induced

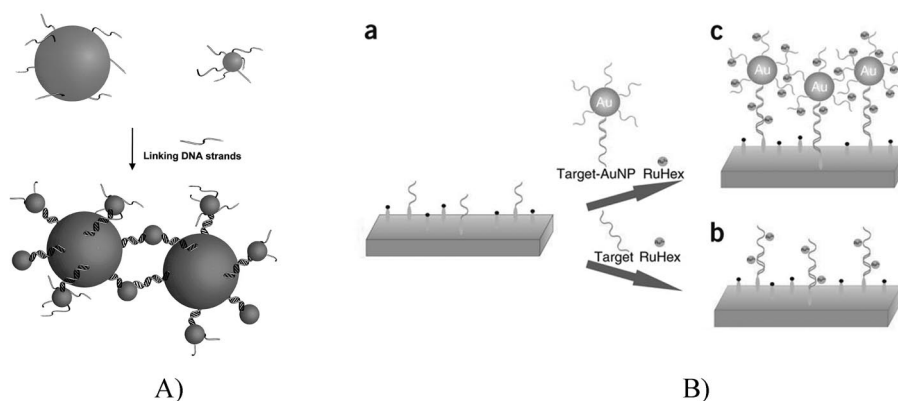


**Fig. 1** AuNP/DNA conjugates-based DNA detection. (A) Colorimetric DNA detection based on the aggregation-induced red-to-blue color change. (Reprinted with permission from ref. [33]. Copyright © 2000 American Chemical Society.); (B) Electrochemical DNA detection with high sensitivity, which relies on the AuNP-based signal amplification [34].

aggregation turns the solution color from red to blue, signaling the presence of the DNA target [25]. This strategy was later significantly improved in sensitivity to match or even exceed that of fluorescent assays, by coupling AuNP nanoprobes with either silver staining or Raman resonance [29–32].

We developed an AuNP-based electrochemical DNA sensor by using AuNP/DNA conjugates [35]. We also employed a “sandwich-type” strategy, which involves capture probe DNA self-assembled at gold electrodes and reporter DNA loaded on AuNPs (Fig. 1B), both of which flank the DNA target sequence. In the presence of target DNA, AuNPs loaded with the reported DNA are brought to the proximity of the electrode surface via the hybridization between the capture probe, the target DNA and the reporter DNA. Since a single AuNP is loaded with hundreds of reporter DNA strands, this offers a significant amplification for the detection of target DNA. We employed a redox probe,  $[\text{Ru}(\text{NH}_3)_6]^{3+}$ , to electrochemically interrogate the hybridization event with AuNP amplification. Because of the significant amplification of AuNPs, our prototype DNA sensor could detect as low as femtomolar (zepto-moles) DNA targets and exhibited excellent selectivity against even a single-base mismatch.

The AuNP-based biodetection strategy can be extended to the detection of a variety of targets aside from DNA molecules, with the introduction of aptamers. Aptamers are DNA or RNA structures possessing high binding affinity to various ligands [36–39], while DNazymes/RNazymes are catalytic nucleic acids exhibiting activities just like protein enzymes [40,41]. These in vitro selected structures have become increasingly important as molecular tools in biotechnology [42], and particularly in the design of various biosensors. AuNP/DNA conjugates are also used as probes for aptamer-based sensing. Lu's group developed a series of sensing strategies for lead ion, adenosine, potassium ion, and cocaine by using such nanoprobes [43–48]. In a typical design for adenosine detection, the aptamer was pre-hybridized with AuNP/DNA conjugates, forming purple-colored aggregates (Fig. 2). Upon the addition of target molecules, the AuNP aggregates were disassembled into red-colored individual AuNPs. This purple-to-red color change served as the visual signal for the target.

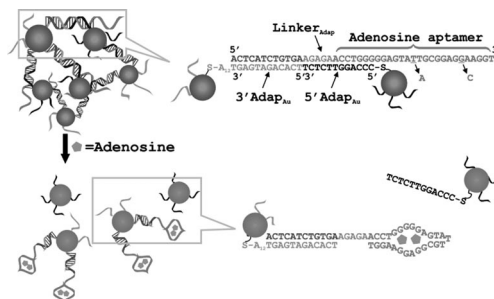


**Fig. 2** AuNP/DNA conjugates for aptamer-based detection. The target-induced disassembly of AuNP aggregates leads to a blue-to-red color change, signaling the presence of the target molecule [49]. (Copyright © Wiley-VCH Verlag GmbH & Co. KGaA. Reproduced with permission.)

Environmentally toxic mercury ions can also be detected with nanoprobes by attaching a mercury-specific T-rich DNA probe to AuNPs, which was developed independently in several laboratories [45,50–54]. We recently designed a microfluidic chip-based assay for rapid and portable mercury detection (Fig. 3). We prepared the Au nanoprobe through modification of AuNPs with thiolated thymine oligonucleotides (a mixture of T6/T10). This structure allows rapid response to  $\text{Hg}^{2+}$  within microfluidic channels and at room temperature. In the presence of  $\text{Hg}^{2+}$ , adjacent thymine probes at the surface of each AuNP formed the T– $\text{Hg}^{2+}$ –T complex. This changed the surface charge distribution and destabilized AuNPs against aggregation at high ionic strength, leading to a red-to-purple color change. The PDMS-based microfluidic device was pre-degassed. When the nanoprobe and the mercury ion-containing sample were injected into two inlets, the pressure difference forced the solution to flow through

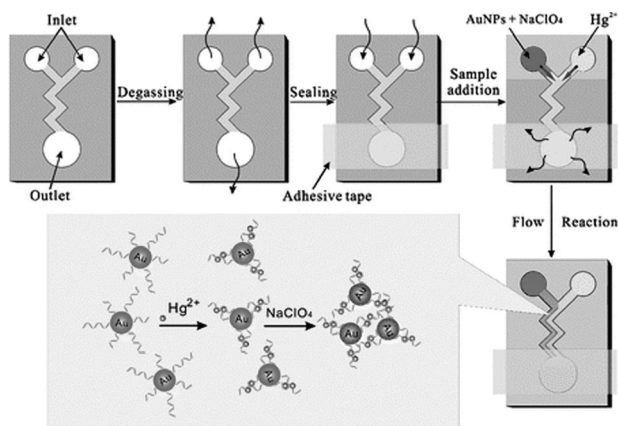


**Fig. 3** Scheme for the power-free  $\text{Hg}^{2+}$  sensing strategy [55]. The black arrows in each step indicate the directions of air transfer. Also shown is the scheme for optical detection of  $\text{Hg}^{2+}$  using thymine-modified Au nanoparticles. (Reproduced by permission of The Royal Society of Chemistry, RSC.)

the channel without external power, leading to a deposition line arising from the AuNPs aggregation. This simple device allows extremely convenient  $\text{Hg}^{2+}$  detection with the naked eye.

Since AuNPs possess a very high surface-to-volume ratio, one may design multifunctional nanoprobes by attaching multiple kinds of biomolecules at the surface of a single particle. An elegant example is Mirkin's "bio-barcode" nanoprobe designed for the highly amplified detection of protein biomarkers [56,57]. They conjugated antibodies on AuNPs encoded with DNA probes that were unique to the target protein. The classic immunological reaction was replaced with the identification of the encoded DNA probes attached to AuNPs. Since each AuNP carried a large number of oligonucleotides corresponding to a protein binding event, substantial amplification was achieved, leading to ultrahigh sensitivity up to the low attomolar detection limit [58].

We recently designed a highly integrated nanoprobe that combined DNA recognition (DNA detection probe), signal amplification (enzyme), and nonspecific blocking within one AuNP (Fig. 4). This multicomponent nanoprobe possessed high hybridization specificity as well as other inherited advantages of DNA-AuNP conjugates, obviating additional (separated) signal amplification steps. The nanoprobe was prepared by assembling AuNPs with DNA detection probe, horse radish peroxidase (HRP), and bovine serum albumin (BSA), where the DNA detection probe was used to construct the

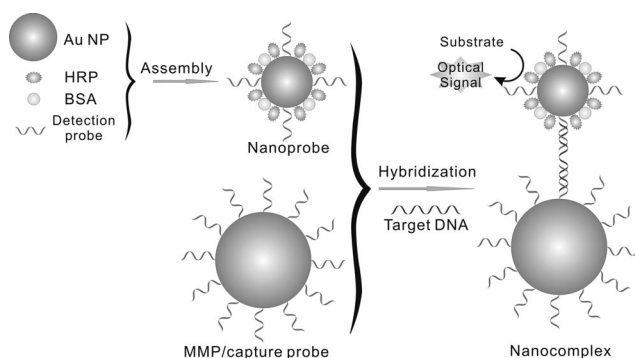


**Fig. 4** Enzyme-based multicomponent nanoprobe for DNA detection [59]. (Copyright © Wiley-VCH Verlag GmbH & Co. KGaA. Reproduced with permission).

sandwich complex, HRP was for enzymatic catalysis, and BSA was a nonspecific blocker. After a “sandwich-type” assay, the capture probe brought the target DNA, along with the detection probe, to the proximity of MMPs, and this complex could be magnetically separated for subsequent optical detection. With this novel multifunctional nanoprobe, we could conveniently detect as few as 100 pM target DNA with the naked eye. This multifunctional strategy was recently extended to the detection proteins by attaching protein-specific aptamers to AuNPs (Li et al., unpublished).

### UNMODIFIED AuNPs AS NANOPROBES

AuNPs without modification of DNA probes can also serve as optical biological probes. The use of unmodified AuNP probe started from the work of Li and Rothberg [58,60,61]. They found that single-stranded DNA (ssDNA) and double-stranded DNA (dsDNA) have different adsorption properties on the surface of AuNPs. Significantly, ssDNA while not dsDNA spontaneously and tightly binds to unmodified AuNPs (Fig. 5), this large affinity difference is associated with the competition of two opposite effects. That is, DNA bases (A, G, T, C) possess high affinity to gold via coordination between Au and nitrogen atoms (favoring DNA adsorption) [61]; in contrast, negatively charged surfaces of AuNPs electrostatically repel DNA phosphate backbones (disfavoring DNA adsorption) [62]. Interestingly, the formation of duplex not only doubles the surface charge density as compared to ssDNA, but also prevents the exposure of DNA bases to Au, thus disfavoring the adsorption of dsDNA on AuNPs in both facets. Moreover, unstructured ssDNA is soft and random-coil-like (with a persistence length of ~1 nm), which is in sharp contrast to the rigid structure of dsDNA (with a persistence length of ~50 nm). As a result, ssDNA has significantly higher freedom to wrap on AuNPs than dsDNA, which might also contribute to the differentiation ability of AuNPs.

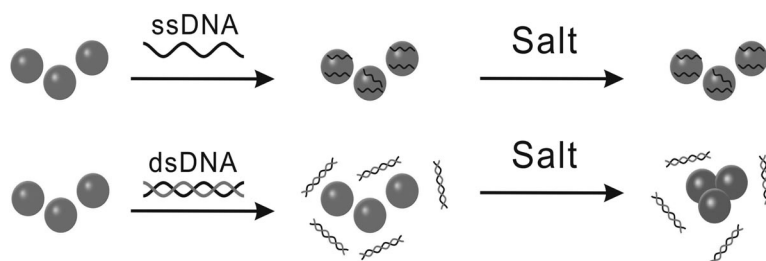


**Fig. 5** DNA detection using unmodified AuNPs. AuNPs effectively differentiate ssDNA and dsDNA, leading to a characteristic red-to-blue color change in response to the DNA hybridization [58].

Based on this novel finding, Li and Rothberg developed a rapid, mix-and-detect assay protocol for the sequence-specific detection of DNA targets [60]. As shown in Fig. 5, the binding of ssDNA on the surface of AuNPs significantly adds the surface charges, thus stabilizing AuNPs from being aggregated in solutions of high ionic strength. In contrast, if the ssDNA probe forms the duplex with its target, AuNPs are not protected and easily aggregated with the salt addition, leading to a characteristic red-to-blue color change that arises from the size-dependent shift of SPR absorption. This color change arising from AuNP aggregation provides a convenient means to visually detect target DNA with unmodified AuNPs. They demonstrated that the assay is very fast (within 5 min) and can detect as few as 100 femtomoles of target without instrumentation [58]. In addition, this assay method is adaptable for the detection of genomic DNA via AuNP-based sensing of polymerase chain reaction (PCR)-generated amplicons [60]. This novel AuNPs-based sensing strategy is label-free, obviating the necessity of either labeling DNA or modification of AuNPs, and kinetically fast, allowing a mix-and-detect assay format. However, the sensitivity is relatively low. This disadvantage can be avoided via introduction of a fluo-

rescent assay protocol, which also relies on the differentiation ability of AuNPs toward ssDNA and dsDNA, and on the quenching ability of AuNPs toward fluorescent dyes [61].

Unmodified AuNPs also serve as a visual probe for ligand-induced aptamer structural variations. We previously demonstrated that unmodified AuNPs could effectively differentiate unstructured and folded aptamers by exploiting interactions between AuNPs and the single-stranded aptamer sequences, based on which we extended the use of AuNPs to the detection of a range of ions and molecules (Fig. 6A) [63]. Our first attempt involved the use of a G-quartet structure that is the aptamer for the potassium ion. Similar to the ssDNA-to-dsDNA change, the formation of G-quartets after the binding of targets disfavors the adsorption between DNA and AuNPs due to the encapsulation of DNA bases and the increase of the rigidity. As a proof-of-concept, we challenged AuNPs with the G-rich aptamer either in the presence or in the absence of  $K^+$ . Upon the addition of salt, the former solution showed a red-to-purple change of color within several minutes, while the latter retained its original red color. Importantly, this characteristic color change exhibited a  $K^+$  concentration-dependent manner, leading to a rapid and convenient assay method for micromolar potassium ion. This strategy was later extended to the detection of mercury ion with a T-rich DNA probe and solution pH with a C-rich DNA probe (termed i-motif) [52]. Both probes underwent a random coil-to-rigid structure change that was translated into the characteristic color change of AuNPs, signaling the environmentally toxic  $Hg^{2+}$  and pH values [50,52]. By using a similar strategy, Dong and co-workers also developed an assay method for the detection of thrombin molecules with a thrombin aptamer [64]. More recently, Zhao et al. developed a rapid colorimetric assays for the enzymatic activity of calf intestine alkaline phosphatase (CIAP) based on the non-cross-linking AuNP aggregation [65].

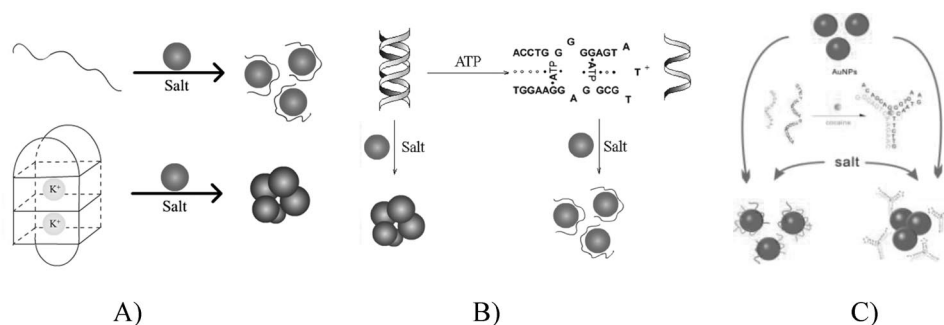


**Fig. 6** Unmodified AuNPs for aptamer-based detection. (A) Unmodified AuNPs recognize the random coil-to-G-quartet structural variation, leading to a red-to-blue color change [63]. (Reproduced with permission of The Royal Society of Chemistry, RSC.); (B) The displacement-based detection strategy. Unmodified AuNPs recognize the dsDNA-to-ssDNA change, leading to a blue-to-red color change [66]. (Copyright © Wiley-VCH Verlag GmbH & Co. KGaA. Reproduced with permission.); (C) The presence of the target molecule glues the two engineered aptamer pieces into an intact structure. Unmodified AuNPs recognize this process, leading to a red-to-blue color change [67]. (Copyright © Wiley-VCH Verlag GmbH & Co. KGaA. Reproduced with permission.)

While the above-mentioned strategy offers a highly convenient approach for aptamer-based detection, the generality of this strategy remains a problem. This is because many aptamers possess inner secondary structures even in the absence of targets, thus the target-induced structural change is insufficient to significantly alter the affinity of aptamers to AuNPs. In order to overcome this shortcoming, we designed an alternative displacement-based strategy that translated an aptamer-target binding event into a duplex-to-aptamer dehybridization process which can be conveniently detected with unmodified AuNPs in a colorimetric approach (Fig 6B) [20]. In this strategy, the target-free aptamer is first hybridized with its complementary sequence to form a rigid duplex. Provided that there is a specific target, the aptamer-target binding disassembled the original duplex to form a tertiary structure and release

an ssDNA strand. We found that unmodified AuNPs could clearly identify this target-induced displacement process via the blue-to-red color change, in a similar way to the method of Li and Rothberg [58]. For example, ATP of micromolar concentration could be easily detected even with naked eyes. Importantly, this strategy does not rely on the specific aptamer structure, thus is highly generic. We also demonstrated the applicability of this strategy in the sensing of potassium ion and cocaine.

More recently, we designed a new bioassay strategy to detect small-molecule targets based on AuNPs and engineered DNA aptamers. We artificially engineered an aptamer into two pieces of random, coil-like ssDNA [67]. We assumed that these two pieces might reassemble into the intact aptamer tertiary structure in the presence of the specific target. By using a cocaine aptamer as the model, we demonstrated that cocaine did assemble two engineered pieces into a rigid structure, and AuNPs could effectively differentiate between these two states via their characteristic surface-plasmon resonance-based color change (Fig. 6C). By using this method, we could selectively detect cocaine of the low-micromolar range and within minutes. This strategy is also fairly generic and applicable to the detection of several other small-molecule targets such as adenosine and potassium. More importantly, compared to the displacement-based strategy, this novel strategy is inherently fast in kinetics since it does not involve competition and the employed sequences are much shorter. Indeed, we found that we could differentiate target binding within several minutes with this strategy (vs. ~30 min with the displacement-based strategy).

## CONCLUSIONS

In this review, we have demonstrated recent progress on the use of two types of nanoprobes, AuNP/DNA conjugates and unmodified AuNPs for the detection of DNA, proteins as well as a range of small-molecule targets. These nanoprobe-based sensing strategies exploit several unique optical and electronic properties of AuNPs, such as SPR, fluorescence quenching, and Raman scattering. Given that AuNPs possess large surface-to-volume ratio, it is also possible to develop multifunctional nanoprobes by attaching various biomolecular probes to the surface of a single AuNP. We expect that such AuNP-based biosensing strategies will find important applications in biomedical diagnostics, environmental monitoring as well as civil defense.

## ACKNOWLEDGMENTS

This work was financially supported by National Project 973 (Grant Nos. 2007CB936000, 2006CB933000), National Natural Science Foundation (Grant Nos. 20704043, 20805055), Shanghai Natural Science Foundation (Grant No. 07ZR14136), Shanghai Rising-star Program (Grant Nos. 08QA14078, 08QH14029), and the K. C. Wong Education Foundation, Hong Kong, China.

## REFERENCES

1. J. Wang. *Small* **1**, 1036 (2005).
2. S. P. Song, L. H. Wang, J. Li, J. L. Zhao, C. Fan. *Trends Anal. Chem.* **27**, 108 (2008).
3. S. K. Ghosh, T. Pal. *Chem. Rev.* **107**, 4797 (2007).
4. G. Schmid. *Clusters and Colloids: From Theory to Applications*, Wiley-VCH, Weinheim (1994).
5. S. K. Ghosh, A. Pal, S. Nath, S. Kundu, S. Panigrahi, T. Pal. *Chem. Phys. Lett.* **412**, 5 (2005).
6. S. K. Ghosh, A. Pal, S. Kundu, S. Nath, T. Pal. *Chem. Phys. Lett.* **395**, 366 (2004).
7. S. Ghosh, S. Kundu, M. Mandal, T. Pal. *Langmuir* **18**, 8756 (2002).
8. S. Hayashi. *Jpn. J. Appl. Phys.* **23**, 665 (1984).
9. J. D. Jackson, R. F. Fox. *Am. J. Phys.* **67**, 841 (1999).
10. S. Chen, R. Pei. *J. Am. Chem. Soc.* **123**, 10607 (2001).
11. A. Henglein. *J. Phys. Chem. B* **104**, 6683 (2000).

12. A. Henglein, M. Giersig. *J. Phys. Chem. B* **104**, 5056 (2000).
13. J. Park, J. Cheon. *J. Am. Chem. Soc.* **123**, 5743 (2001).
14. S. Park, P. Yang, P. Corredor, M. Weaver. *J. Am. Chem. Soc.* **124**, 2428 (2002).
15. Z. Zhong, K. Male, J. Luong. *Anal. Lett.* **36**, 3097 (2003).
16. Z. Wang. *J. Phys. Chem. B* **104**, 1153 (2000).
17. J. Krug, G. Wang, S. Emory, S. Nie. *J. Am. Chem. Soc.* **121**, 9208 (1999).
18. A. Templeton, M. Hostetler, E. Warmoth, S. Chen, C. Hartshorn, V. Krishnamurthy, M. Forbes, R. Murray. *J. Am. Chem. Soc.* **120**, 4845 (1998).
19. A. P. Alivisatos, K. P. Johnsson, X. G. Peng, T. E. Wilson, C. J. Loweth, M. P. Bruchez, P. G. Schultz. *Nature* **382**, 609 (1996).
20. C. A. Mirkin, R. L. Letsinger, R. C. Mucic, J. J. Storhoff. *Nature* **382**, 607 (1996).
21. M. M. Alvarez, J. T. Houry, T. G. Schaaff, M. N. Shafiqullin, I. Vezmar, R. L. Whetten. *J. Phys. Chem. B* **101**, 3706 (1997).
22. P. Englebienne. *Spectroscopy* **17**, 255 (2003).
23. W. Zhao, M. A. Brook, Y. Li. *ChemBioChem* **9**, 2363 (2008).
24. M. C. Daniel, D. Astruc. *Chem. Rev.* **104**, 293 (2004).
25. R. Elghanian, J. J. Storhoff, R. C. Mucic, R. L. Letsinger, C. A. Mirkin. *Science* **277**, 1078 (1997).
26. L. M. Demers, C. A. Mirkin, R. C. Mucic, R. A. Reynolds 3<sup>rd</sup>, R. L. Letsinger, R. Elghanian, G. Viswanadham. *Anal. Chem.* **72**, 5535 (2000).
27. R. Jin, G. Wu, Z. Li, C. Mirkin, G. Schatz. *J. Am. Chem. Soc.* **125**, 1643 (2003).
28. T. A. Taton, C. A. Mirkin, R. L. Letsinger. *Science* **289**, 1757 (2000).
29. Y. C. Cao, R. Jin, C. A. Mirkin. *Science* **297**, 1536 (2002).
30. J. Zhang, S. Song, L. Zhang, L. Wang, H. Wu, D. Pan, C. Fan. *J. Am. Chem. Soc.* **128**, 8575 (2006).
31. N. L. Rosi, C. A. Mirkin. *Chem. Rev.* **105**, 1547 (2005).
32. S. J. Park, T. A. Taton, C. A. Mirkin. *Science* **295**, 1503 (2002).
33. C. A. Mirkin. *Inorg. Chem.* **39**, 2258 (2000).
34. J. Zhang, S. Song, L. Wang, D. Pan, C. Fan. *Nat. Protoc.* **2**, 2888 (2007).
35. M. Famulok. *Curr. Opin. Struct. Biol.* **9**, 324 (1999).
36. A. D. Ellington, J. W. Szostak. *Nature* **346**, 818 (1990).
37. T. Hermann, D. J. Patel. *Science* **287**, 820 (2000).
38. C. Tuerk, L. Gold. *Science* **249**, 505 (1990).
39. G. F. Joyce. *Annu. Rev. Biochem.* **73**, 791 (2004).
40. Y. Li, R. R. Breaker. *Curr. Opin. Struct. Biol.* **9**, 315 (1999).
41. R. R. Breaker. *Curr. Opin. Chem. Biol.* **1**, 26 (1997).
42. S. Fredriksson, M. Gullberg, J. Jarvius, C. Olsson, K. Pietras, S. M. Gustafsdottir, A. Ostman, U. Landegren. *Nat. Biotechnol.* **20**, 473 (2002).
43. J. Liu, D. Mazumdar, Y. Lu. *Angew. Chem., Int. Ed.* **45**, 7955 (2006).
44. D. G. Georganopoulou, L. Chang, J. M. Nam, C. S. Thaxton, E. J. Mufson, W. L. Klein, C. A. Mirkin. *Proc. Natl. Acad. Sci. USA* **102**, 2273 (2005).
45. J. Liu, Y. Lu. *Angew. Chem., Int. Ed.* **46**, 7587 (2007).
46. J. Liu, Y. Lu. *Nat. Protoc.* **1**, 246 (2006).
47. J. Liu, Y. Lu. *J. Am. Chem. Soc.* **126**, 12298 (2004).
48. J. Liu, Y. Lu. *J. Am. Chem. Soc.* **125**, 6642 (2003).
49. J. Liu, Y. Lu. *Angew. Chem., Int. Ed.* **45**, 90 (2006).
50. D. Li, A. Wieckowska, I. Willner. *Angew. Chem., Int. Ed.* **47**, 3927 (2008).
51. Z. Wang, J. H. Lee, Y. Lu. *Chem. Commun.* 6005 (2008).
52. L. Wang, J. Zhang, X. Wang, Q. Huang, D. Pan, S. Song, C. Fan. *Gold Bull.* **41**, 37 (2008).
53. X. Liu, H. Wu, Y. Li, Q. Li, L. Wang. *Nucl. Sci. Tech.* **30**, 467 (2007).
54. X. Xue, F. Wang, X. Liu. *J. Am. Chem. Soc.* **130**, 3244 (2008).

55. S. He, D. Li, C. Zhu, S. Song, L. Wang, Y. Long, C. Fan. *Chem. Commun.* 4885 (2008).
56. B. Oh, J. Nam, S. Lee, C. Mirkin. *Small* **2**, 103 (2006).
57. J. M. Nam, C. S. Thaxton, C. A. Mirkin. *Science* **301**, 1884 (2003).
58. H. Li, L. Rothberg. *Proc. Natl. Acad. Sci. USA* **101**, 14036 (2004).
59. J. Li, S. Song, X. Liu, L. Wang, D. Pan, Q. Huang, Y. Zhao, C. Fan. *Adv. Mater.* **20**, 497 (2008).
60. H. Li, L. J. Rothberg. *J. Am. Chem. Soc.* **126**, 10958 (2004).
61. H. Li, L. J. Rothberg. *Anal. Chem.* **76**, 5414 (2004).
62. L. M. Demers, M. Ostblom, H. Zhang, N.-H. Jang, B. Liedberg, C. A. Mirkin. *J. Am. Chem. Soc.* **124**, 11248 (2002).
63. L. Wang, X. Liu, X. Hu, S. Song, C. Fan. *Chem. Commun.* 3780 (2006).
64. H. Wei, B. Li, J. Li, E. Wang, S. Dong. *Chem. Commun.* 3735 (2007).
65. W. Zhao, W. Chiuman, J. C. F. Lam, M. A. Brook, Y. Li. *Chem. Commun.* 3729 (2007).
66. J. Wang, L. H. Wang, X. F. Liu, Z. Q. Liang, S. P. Song, W. X. Li, G. X. Li, C. Fan. *Adv. Mater.* **19**, 3943 (2007).
67. J. Zhang, L. Wang, D. Pan, S. Song, F. Y. Boey, H. Zhang, C. Fan. *Small* **4**, 1196 (2008).